Effect of Single-Site Charge-Reversal Mutations on the Catalytic Properties of Yeast Cytochrome *c* Peroxidase: Evidence for a Single, Catalytically Active, Cytochrome *c* Binding Domain[†]

Naw May Pearl, Timothy Jacobson, Cassandra Meyen, Anthony G. Clementz, Esther Y. Ok, Eric Choi, Kyle Wilson, Lidia B. Vitello, and James E. Erman*

Department of Chemistry and Biochemistry, Northern Illinois University, DeKalb, Illinois 60115

Received November 14, 2007; Revised Manuscript Received January 10, 2008

ABSTRACT: Forty-six charge-reversal mutants of yeast cytochrome *c* peroxidase (CcP) have been constructed in order to determine the effect of localized charge on the catalytic properties of the enzyme. The mutants include the conversion of all 20 glutamate residues and 24 of the 25 aspartate residues in CcP, one at a time, to lysine residues. In addition, two positive-to-negative charge-reversal mutants, R31E and K149D, are included in the study. The mutants have been characterized by absorption spectroscopy and hydrogen peroxide reactivity at pH 6.0 and 7.5 and by steady-state kinetic studies using recombinant yeast iso-1 ferrocytochrome *c* (C102T) as substrate at pH 7.5. Many of the charge-reversal mutations cause detectable changes in the absorption spectrum of the enzyme reflecting increased amounts of hexacoordinate heme compared to wild-type CcP. The increase in hexacoordinate heme in the mutant enzymes correlates with an increase in H_2O_2-inactive enzyme. The maximum velocity of the mutants decreases with increasing hexacoordination of the heme group. Steady-state velocity studies indicate that 5 of the 46 mutations (R31E, D34K, D37K, E118K, and E290K) cause large increases in the Michaelis constant indicating a reduced affinity for cytochrome *c*. Four of the mutations occur within the cytochrome *c* binding site identified in the crystal structure of the 1:1 complex of yeast cytochrome *c* and CcP [Pelletier, H., and Kraut, J. (1992) *Science 258*, 1748–1755] while the fifth mutation site lies outside, but near, the crystallographic site. These data support the hypothesis that the CcP has a single, catalytically active cytochrome *c* binding domain, that observed in the crystal structures of the cytochrome *c*/CcP complex.

Cytochrome *c* peroxidase (CcP)[1] catalyzes the reduction of hydrogen peroxide to water using ferrocytochrome *c* (*1*). The catalytic mechanism involves oxidation of the native enzyme by hydrogen peroxide to an enzyme intermediate called CcP Compound I (CcP-I) (eq 1). CcP-I is reduced back to the native state via a second intermediate, CcP Compound II (CcP-II), by two sequential electron transfer steps from ferrocytochrome *c* (eqs 2 and 3).

$$\mathrm{CcP} + \mathrm{H_2O_2} \rightarrow \mathrm{CcP\text{-}I} + \mathrm{H_2O} \quad (1)$$

$$\mathrm{CcP\text{-}I} + \mathrm{C^{2+}} \rightarrow \mathrm{CcP\text{-}II} + \mathrm{C^{3+}} \quad (2)$$

$$\mathrm{CcP\text{-}II} + \mathrm{C^{2+}} \rightarrow \mathrm{CcP} + \mathrm{C^{3+}} + \mathrm{H_2O} \quad (3)$$

In eqs 2 and 3, C^{2+} and C^{3+} represent ferro- and ferricytochrome *c*, respectively. CcP-I contains two oxidized sites, an oxyferryl Fe(IV) heme group and a tryptophan π-cation radical located within van der Waals distance of the heme. Steps 2 and 3 of the catalytic mechanism involve binding of, and electron transfer from, ferrocytochrome *c*. The number, location, affinity, and electron transfer activity of the cytochrome *c* binding sites on the surface of CcP are still unresolved (*2, 3*).

Margoliash and co-workers were the first to suggest the possibility of multiple cytochrome *c* binding sites on the surface of CcP in 1977 (*4*). They observed biphasic steady-state velocity profiles as a function of the cytochrome *c* concentration and interpreted their results on the basis of formation of both 1:1 and 2:1 cytochrome *c*/CcP complexes. Since that time a large number of studies have been published concerning the nature of the cytochrome *c*/CcP interaction and the potential locations of the cytochrome *c* binding sites on CcP (*5–28*). There is general agreement that both 1:1 and

[†] This work was supported in part by a grant from the National Institutes of Health (R15 GM59740).

* Corresponding author. Phone: (815) 753-6867. Fax: (815) 753-4802. E-mail: jerman@niu.edu.

[1] Abbreviations: CcP, generic abbreviation for cytochrome *c* peroxidase whatever the source; yCcP, yeast cytochrome *c* peroxidase isolated from bakers' yeast, *Saccharomyces cervisiae*; rCcP, recombinant CcP expressed in *Escherichia coli* with an identical amino acid sequence as yCcP; CcP(MI), recombinant CcP expressed in *E. coli* with four amino acid variations compared to yCcP, a Met-Ile N-terminal extension and mutations T53I and D152G; CcP-I, CcP Compound I, the first intermediate observed in the catalytic cycle produced upon oxidation of CcP with hydrogen peroxide; CcP-II, CcP Compound II, the second intermediate observed in the catalytic cycle produced by one-electron reduction of CcP-I; CcP-II_F, CcP Compound II in which the oxidized site is Fe(IV); CcP-II_R, CcP Compound II in which the oxidized site is the Trp-191 radical; C^{2+}, ferrocytochrome *c*; C^{3+}, ferricytochrome *c*. Mutations in the amino acid sequences of either CcP or cytochrome *c* are indicated by using the one letter code for the amino acid residue in the wild-type protein, followed by the residue number and the one letter code for the amino acid residue in the mutant protein; i.e., C102T represents a mutant in which a threonine residue replaces the cysteine residue at position 102 of the wild-type protein.

10.1021/bi702271r CCC: $40.75 © 2008 American Chemical Society
Published on Web 01/31/2008

2:1 cytochrome *c*/CcP complexes exist in solution, that formation of both complexes is dependent upon the ionic strength with strongest binding occurring at low ionic strength, and that formation of the 1:1 complex is about 10^3 times stronger than formation of the 2:1 complex.

Two general binding models have been proposed for binding of cytochrome *c* to CcP. The first is a unique site model in which there is a single high-affinity cytochrome *c* binding site and a much weaker secondary cytochrome *c* binding site. The unique site model is supported by crystal structures of several 1:1 cytochrome *c*/CcP complexes that show cytochrome *c* binding to the same general area on the surface of CcP (*5, 26–28*). The second model proposes that there are several binding sites on CcP with similar affinities for cytochrome *c*. Multiple 1:1 cytochrome *c*/CcP complexes can exist in solution, each differing by the location of the bound cytochrome and their relative abundance determined by the binding affinities at each site. In this model, formation of the 2:1 complex is much weaker due to strong electrostatic repulsion between bound cytochromes in the 2:1 complex. The multiple, interacting site model is supported by computer simulations of the interaction between the two proteins (*7*) and by chemical modification of CcP in the presence and absence of bound cytochrome *c* (*11*).

Site-directed mutagenesis of CcP has been used to test suggested locations for the cytochrome *c* binding sites (*14–20*). However, the studies published to date are incomplete in that all potential cytochrome *c* binding sites may not have been identified through theoretical studies or tested experimentally. We have initiated a systematic study to identify all of the negatively charged groups on CcP that influence formation of both the 1:1 and 2:1 yeast iso-1 cytochrome *c*/CcP complexes. If there is a single high-affinity binding site, the charge-reversal mutations that affect formation of the 1:1 complex should be clustered near the binding site identified in the crystal structures of the cytochrome *c*/CcP complex (*5, 26–28*). However, if there are multiple binding sites with similar affinities for cytochrome *c*, then charge-reversal mutations located more distant from the crystallographic site will affect formation of the 1:1 complex. Likewise, determining the negatively charged residues on the surface of CcP that affect formation of the 2:1 complex will locate at least two binding regions for cytochrome *c*.

We have mutated, individually, every aspartate and glutamate residue on the surface of CcP to a lysine residue. In addition, we have constructed two internal aspartate to lysine mutants, D76K and D235K, and two positive-to-negative charge reversal mutants, R31E and K149D, providing a library of 46 charge-reversal mutants that will be useful in identifying the cytochrome *c* binding sites and to investigate the effect of localized charge on the properties of CcP.

In a previous report (*29*), we presented initial characterization of 15 charge-reversal mutants in which the site of mutation was located near the crystallographically defined binding site (*5, 26–28*). In this report, we complete the characterization of all 46 charge-reversal mutants using UV–visible spectroscopy, hydrogen peroxide reactivity, and steady-state kinetic studies of the CcP-catalyzed oxidation of yeast iso-1 ferrocytochrome *c* (C102T) by H_2O_2.

MATERIALS AND METHODS

All relevant experimental protocols have been described in detail in the previous report on this investigation (*29*). Briefly, the expression system for the recombinant CcP (rCcP) was provided by James Satterlee, Washington State University (*30*). The cloned gene has a sequence identical to that of mature baker's yeast CcP (yCcP) with the exception of the methionine codon required for bacterial expression (*31*). The N-terminal methionine is removed from rCcP in this expression system, producing a recombinant enzyme identical to yCcP (*32*). Gary Pielak, University of North Carolina at Chapel Hill, provided the plasmid pBTR(C102T) containing the gene for yeast iso-1 cytochrome *c* (C102T) used in this study (*33*). Cys-102 in yeast iso-1 cytochrome *c* has been replaced with threonine (C102T) to prevent dimerization of the native protein via disulfide bond formation. The plasmid also contains the gene for yeast cytochrome *c* heme lyase to promote covalent attachment of the heme (*34*). Mutations in CcP were created using Stratagene QuikChange mutagenesis kits.

Protein expression, purification, and concentration determinations have been described previously (*29*). Spectra were determined using either a Hewlett-Packard Model 8452A diode array spectrophotometer or a Varian/Cary Model 3E spectrophotometer.

The rates of the reaction between hydrogen peroxide and the mutant enzymes were determined using an APL Ltd. model SX.17MV stopped-flow spectrofluorometer. Reactions were carried out in 0.100 M ionic strength potassium phosphate buffer, at both pH 6.0 and pH 7.5, 25 °C. Rates were measured under pseudo-first-order conditions with H_2O_2 in excess, 3−18 μM. The fraction of H_2O_2-active enzyme was estimated by comparing the spectrum of the hydrogen peroxide-oxidized mutant to that of authentic yCcP Compound I. Steady-state kinetic studies of the enzyme-catalyzed oxidation of yeast iso-1 ferrocytochrome *c* (C102T) by H_2O_2 were performed at pH 7.5 using 0.100 M ionic strength potassium phosphate buffer. Steady-state velocities were measured over a range of ferrocytochrome *c* concentrations, 1−100 μM, at constant 200 μM H_2O_2. Enzyme concentrations were generally between 1 and 10 nM for the steady-state kinetic experiments. For the inactive mutants, i.e., CcP(D235K) and CcP(E267K), enzyme concentrations of up to 1 μM were used.

RESULTS AND DISCUSSION

Location of Charge-Reversal Mutation Sites. The crystal structures of nine different cytochrome *c*/CcP complexes have been published to date with their coordinates deposited in the Protein Data Bank (*5, 26–28*). In all cases, cytochrome *c* binds to the same general region on the surface on CcP as shown in Figure 1, and we have defined this surface as the "front face" of CcP (*29*). We also define the "right face" and "left face" of CcP by 90° rotations about a vertical axis in the clockwise and counterclockwise directions, respectively, while a 180° rotation from the front face reveals the "back face" of CcP. Table 1 lists the 44 surface mutants used in this study with respect to their location on the four faces of CcP. The two internal mutants, E76K and D235K, are not included in Table 1. Figures of the four faces of CcP

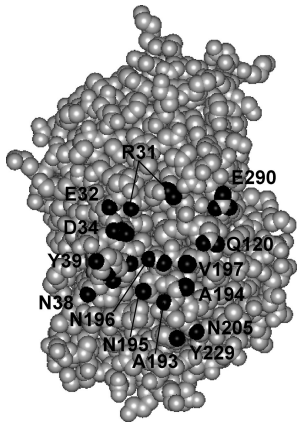

FIGURE 1: Cytochrome *c* footprint on the surface of CcP. Nine crystal structures of various cytochrome *c*/cytochrome *c* peroxidase complexes have been reported with their coordinates deposited in the Protein Data Bank (*5, 26–28*). The PDB IDs are 2pcb, 2pcc, 1u74, 1u75, 2b0Z, 2b10, 2b11, 2b12, and 2bcn. Only 25 atoms on the surface of CcP, residing in 14 residues, are within 3.4 Å of an atom in cytochrome *c* in at least one of the nine structures. The 25 atoms are shown in black, and the 14 residues are labeled.

Table 1: Location of the Charge-Reversal Mutants on the Four Faces of CcP[a]

front face	left face	right face	back face
E17K	D37K	E167K	E11K
D18K	D79K	E250K	D58K
R31E[b]	E93K	D254K	D61K
E32K	D132K	D256K	D140K
D33K	E135K	D261K	D146K
D34K	D136K	E267K	D148K
E35K	E188K	E271K	K149D[b]
E98K	E214K		D150K
E118K	D217K		D152K
E201K	D224K		D165K
E209K			E221K
D210K			D241K
E290K			D279K
E291K			

[a] The front face of CcP is defined as the surface that contains the cytochrome *c* binding domain identified in nine different crystal structures of the 1:1 cytochrome *c*/CcP complex (*5, 26–28*). The right face and left face of CcP are defined by 90° rotations about a vertical axis in the clockwise and counterclockwise directions, respectively, while a 180° rotation from the front face reveals the back face of CcP. Two mutants with internal mutation sites, E76K and D235K, are not listed in the table. [b] Positive-to-negative mutations.

with the mutation sites identified are included in the Supporting Information.

Spectroscopic Properties of the Charge-Reversal Mutants. UV–visible absorption spectroscopy was used for the initial characterization of the mutants. Spectra were determined at pH 6.0, the center of the pH stability region for CcP, and at pH 7.5, the pH at which kinetic studies were performed. Spectra for all 46 rCcP mutants at both pH 6.0 and pH 7.5 are shown in the Supporting Information. Selected spectroscopic parameters, including the ratio of absorbance at the Soret maximum to the absorbance at the maximum of the protein band near 280 nm, at pH 6.0, the wavelength of the Soret maximum at both pH 6.0 and pH 7.5, and the ratio of the absorbance at the Soret maximum to that at 380 nm, A_{Soret}/A_{380}, at both pH 6.0 and pH 7.5, are included in Table S1 of the Supporting Information.

The $A_{Soret}/A_{protein}$ value is often used as a measure of heme protein purity since nonheme proteins will contribute to the absorbance near 280 nm but not in the Soret band. We use it here to monitor heme reconstitution and changes in heme coordination of the charge-reversal mutants. The $A_{Soret}/A_{protein}$ values for all 46 mutants at pH 6 are plotted in order of the sequence position in Figure 2. Forty-two of the 46 mutants have $A_{Soret}/A_{protein}$ values between 1.18 and 1.37 with a mean and standard deviation of 1.28 ± 0.04. The $A_{Soret}/A_{protein}$ values for these mutants are consistent with the $A_{Soret}/A_{protein}$ values for multiple isolations of rCcP and yCcP done in our laboratory. The $A_{Soret}/A_{protein}$ values for 6 preparations of rCcP and the last 20 isolations of yCcP both average 1.28 ± 0.03, ranging between 1.22 and 1.32. There are four significant outliers in Figure 2. Three of the mutants, E11K, E118K, and E201K have significantly smaller $A_{Soret}/A_{protein}$ values than rCcP while E267K has a significantly higher $A_{Soret}/A_{protein}$ value.

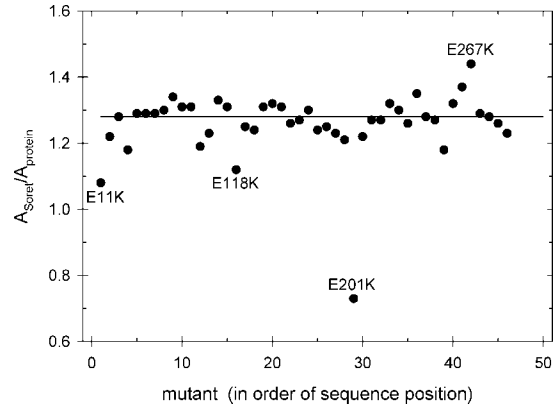

FIGURE 2: Plot of $A_{Soret}/A_{protein}$, the ratio of the absorbance at the Soret maximum to that at the maximum of the protein band, for 46 charge-reversal mutants in order of primary sequence position of the mutation. yCcP has an average $A_{Soret}/A_{protein}$ value of 1.28 ± 0.03 (20 isolations), which is shown by the solid line. Four mutants, E11K, E118K, E201K, and E267K, with the greatest deviation from 1.28 are labeled. The low $A_{Soret}/A_{protein}$ values are attributed to incomplete incorporation of heme, and the high $A_{Soret}/A_{protein}$ value is attributed to a change in heme ligation.

The smaller $A_{Soret}/A_{protein}$ values for E11K, E118K, and E201K are attributed to incomplete heme incorporation into the apoenzyme during the isolation process rather than the copurification of a nonheme protein impurity. On the basis of the $A_{Soret}/A_{protein}$ values, the samples of E11K, E118K, and E201K contain approximately 24%, 12%, and 43% apoprotein, respectively. The apoenzyme does not interfere with the determination of the kinetic properties of these mutants since the concentration of active enzyme is based upon the heme content and only the holoenzyme will react with hydrogen peroxide in the kinetic studies. In the steady-state kinetic studies, the apoenzyme may bind cytochrome *c*, but since the catalytic amounts of apoenzyme, and the amount of cytochrome *c* bound to the apoenzyme, are in the nanomolar concentration region, this will have an insignificant effect on the concentration of free ferrocytochrome *c* and how the ferrocytochrome *c* interacts with the holoenzyme.

The increase in $A_{Soret}/A_{protein}$ for E267K is related to a change in heme coordination. The spectra of rCcP and E267K are shown in Figure 3. The spectrum of rCcP is characteristic of a five-coordinate heme group while the spectrum of E267K is typical for a predominantly six-coordinate, low-spin heme. The extinction coefficient at the Soret maximum of six-coordinate heme is generally larger

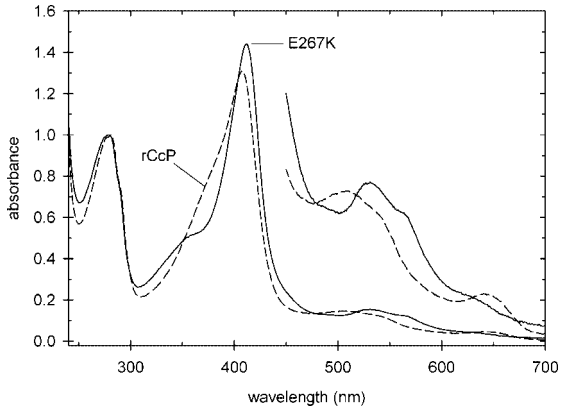

FIGURE 3: Spectrum of E267K (solid line) compared to that of rCcP (dashed line) at pH 6.0. Both spectra are normalized to the maximum in the protein band near 280 nm. The spectrum of E267K has a higher fraction of 6c-ls heme than rCcP as exemplified by the lower absorptivity in the δ band near 350 nm for E267K and near 380 nm for rCcP. The absorbance values in the visible region of the spectra have been multiplied by a factor of 5.

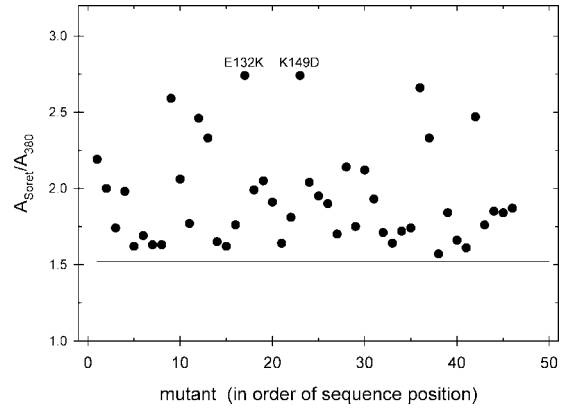

FIGURE 4: Plot of A_{Soret}/A_{380} ratio at pH 7.5 for 46 charge-reversal mutants in order of primary sequence position of the mutation. The A_{Soret}/A_{380} ratio for 100% 5c-hs yCcP is 1.52 ± 0.04 and is shown by the solid line. Values of A_{Soret}/A_{380} above 1.52 represent increasing contributions from hexacoordinate heme species. Two mutants, E132K and K149D, have the largest values for A_{Soret}/A_{380} ratio observed in this study, a value of 2.74.

than for five-coordinate hemes, leading to the higher $A_{Soret}/A_{protein}$ value for E267K compared to rCcP.

Spectroscopic Properties and Heme Ligation. Spectra of heme proteins are sensitive to the redox state, ligation state, and configuration of the *d* electrons in the heme iron (*35–38*). Generally, the spectra of Fe(III) heme proteins can be classified into three groups based on the properties of the heme iron: five-coordinate, high-spin (5c-hs), six-coordinate, high-spin (6c-hs), and six-coordinate, low-spin (6c-ls). Heme proteins can also have equilibrium mixtures of these three states. Wild-type CcP is a predominantly 5c-hs between pH 4 and pH 7 and is characterized by a Soret maximum near 408 nm, prominent charge transfer bands in the visible region of the spectrum near 645 and 505 nm, with the α and β bands appearing as shoulders near 590 and 544 nm, respectively, and the δ band appearing as a very distinct shoulder on the Soret band near 380 nm (Figure 3). Addition of a sixth ligand can generate a high-spin or low-spin heme iron depending upon the field strength of the ligand (*35–38*). In a 6c-hs heme protein spectrum, all heme bands will be blue shifted relative to the 5c-hs spectrum, with an increase in the extinction coefficient at the Soret maximum and a decrease in the extinction coefficient of the δ band. The major spectroscopic changes that occur on going from a 5c-hs heme to a 6c-ls heme include a red shift and increase in extinction coefficient of the Soret band and loss of absorptivity in the charge transfer and δ bands. The spectrum of E267K shown in Figure 3 is typical of a predominantly 6c-ls heme protein. The most consistent changes on going from a five-coordinate heme to a six-coordinate heme, whether high spin or low spin, are the increase in extinction coefficient at the Soret maximum and the loss of absorptivity in the δ band. We have used the ratio of the absorbance at the Soret maximum to the absorbance at 380 nm, A_{Soret}/A_{380}, as a monitor of changes in heme coordination in CcP and the charge-reversal mutants.

At pH 6.0, the A_{Soret}/A_{380} values for yCcP and rCcP are 1.52 ± 0.04 (*20*) and 1.60 ± 0.05 (*6*), respectively (Table S1, Supporting Information). The slightly larger value for rCcP may indicate that rCcP has a slightly greater tendency to form six-coordinate heme than yCcP although the change is small and not much larger than the standard deviation in determining the absorbance ratio.

The charge-reversal mutants have a reasonably large spread in the A_{Soret}/A_{380} values, ranging between 1.44 and 2.53 at pH 6.0 and between 1.57 and 2.74 at pH 7.5 (Table S1, Supporting Information). The pH 7.5 data are shown in Figure 4. The average value of A_{Soret}/A_{380} for all 46 mutants is 1.67 ± 0.19 at pH 6.0 and 1.91 ± 0.31 at pH 7.5 (Table S1, Supporting Information), indicating that the charge-reversal mutants tend to have higher fractions of six-coordinate heme than wild-type enzyme and that the fraction of six-coordinate heme increases with increasing pH.

The spectra of yCcP, CcP(MI), and rCcP are independent of pH between pH 4 and about pH 7 in the absence of buffer components that bind in the heme pocket such as high concentration of acetate and nitrate (*39–41*). The heme group of CcP is predominantly 5c-hs between pH 4 and pH 7. Above pH 7.5, Yonetani et al. observed that the Soret band is red shifted, with increased absorbance at the α and β band positions and decreased absorbance in the charge transfer bands, consistent with conversion to a 6c-ls heme (*39*). These changes are associated with a complex series of transformations at alkaline pH leading to two distinct low-spin forms of CcP, followed by complete denaturation of the enzyme at pH 12 (*42, 43*). The low-spin forms of CcP have absorption spectra that are consistent with a hydroxy-ligated heme and a bisimidazole form of heme. For the latter species, it has been suggested that the polypeptide chain has enough flexibility at alkaline pH to allow the distal histidine, His-52, to coordinate to the heme iron (*43*). The five- and six-coordinate species exist in a pH-dependent equilibrium with apparent pK_A's of 9.7 ± 0.2 and 8.7 ± 0.2 (*41, 42*).

Since most of the charge-reversal mutants have larger fractions of six-coordinate heme than either yCcP or rCcP at pH 7.5, we suggest that the charge-reversal mutations perturb the apparent pK_A's for formation of the 6c-ls species. For hydroxy-ligated CcP this can be rationalized on the basis of electrostatic considerations. The heme group in the 5c-hs form of CcP has a net charge of +1 (neglecting the propionate substituents) resulting from Fe(III) binding into the ring of the porphyrin dianion. Hydroxide binding to the heme iron at alkaline pH neutralizes the net charge at the

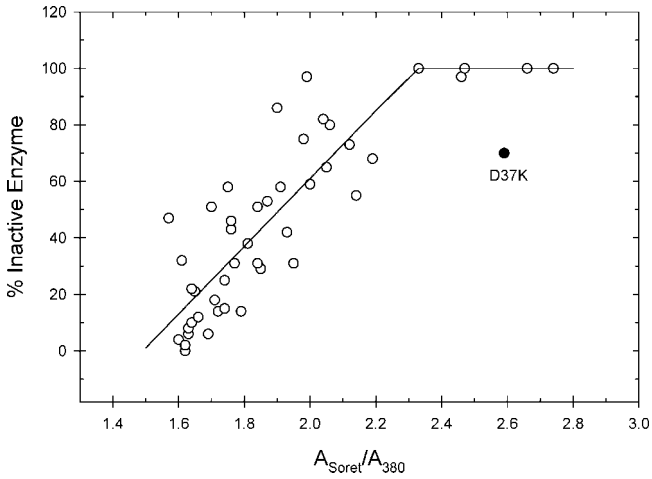

FIGURE 5: Plot of A_{Soret}/A_{380} versus the percentage of H_2O_2-inactive enzyme for 46 charge-reversal mutants of rCcP at pH 7.5. The percentage of H_2O_2-inactive enzyme was estimated from the absorbance change at 424 nm upon addition of a slight stoichiometric excess of hydrogen peroxide. The datum for D37K is labeled and shown as a solid point. The properties of D37K are discussed in the text.

heme core. Electrostatic interactions are long range in nature, and changing a charge on the surface of the protein from −1 to +1 would tend to destabilize the positively charged heme in 5c-hs CcP relative to hydroxide-ligated CcP, leading to lower values of the apparent pK_A for the 5c-hs/6c-ls equilibrium and higher concentrations of the six-coordinate forms at pH 7.5 (Figure 4).

Estimation of the Fraction of H_2O_2-Reactive Enzyme for the Charge-Reversal Mutants. There is an inverse correlation between the H_2O_2 titer of yCcP and the fraction of 6c-ls heme in yCcP, indicating that the 6c-ls forms of the enzyme do not react with H_2O_2 to form CcP Compound I (*41*). In our previous report on 15 of the charge-reversal mutants (*29*), we noted that most of the mutants did not react stoichiometrically with H_2O_2, especially at pH 7.5. Figure 5 shows a correlation of the percentage of H_2O_2-inactive enzyme as a function of the A_{Soret}/A_{380} value, using the latter parameter as a monitor of the six-coordinate heme in the charge-reversal mutants.

In general, the percentage of H_2O_2-inactive enzyme increases as the value of A_{Soret}/A_{380} increases (Figure 5). Mutants with A_{Soret}/A_{380} values between about 1.5 and 2.2 appear to be mixtures of H_2O_2-active and H_2O_2-inactive species while mutants with A_{Soret}/A_{380} values above 2.3 are completely inactive, except for the D37K mutant, which is a conspicuous outlier. The correlation between A_{Soret}/A_{380} is not perfect for a number of reasons. First, the A_{Soret}/A_{380} does not represent conversion of the five-coordinate wild-type enzyme to a single six-coordinate, low-spin species with a specific H_2O_2 reactivity. This is readily apparent with mutants having high A_{Soret}/A_{380} values. Both D79K and D241K have A_{Soret}/A_{380} values of 2.33 and are effectively 100% inactive while both D132K and K149D have A_{Soret}/A_{380} values of 2.74 and are also 100% inactive. The different A_{Soret}/A_{380} values could reflect differences in the sixth ligand. There are at least three potential six-coordinate forms of CcP with either water, hydroxide, or His-52 bound to the heme iron. Each of these three six-coordinate forms will have different A_{Soret}/A_{380} values. While it has not been possible to obtain accurate spectra of the alkaline forms of yCcP due to complex kinetic behavior at pH values greater than 9 (*42*), the two six-coordinate forms of the D235N mutant of CcP(MI) observed between pH 5 and pH 8 have A_{Soret}/A_{380} values of about 2.5 and 3.3 (*43*). The species with A_{Soret}/A_{380} of 2.5 has been assigned to the hydroxy-ligated form and the species with A_{Soret}/A_{380} of 3.3 to the His-52 coordinated form.

The possibility of water existing as the sixth ligand could also lead to variation in the correlation between A_{Soret}/A_{380} and the percentage of active enzyme. Water is an intermediate field ligand, and in many heme proteins, water coordination leads to an equilibrium mixture of high- and low-spin heme (*37*). It is expected that water ligation would increase A_{Soret}/A_{380} over the 5c-hs form but it may not completely inactivate the enzyme. For example, metmyoglobin has a water molecule bound at the sixth coordination site of the heme, yet it still reacts with hydrogen peroxide (*44*). This may be the reason that D37K is an outlier in the correlation shown in Figure 4. Although Asp-37 is a surface residue in CcP, the carboxylate group of Asp-37 hydrogen bonds to His-181 in the interior of the protein. His-181 is part of a hydrogen-bonding network that extends from the proximal heme pocket to the distal heme pocket and includes water-595 (identified in the crystal structure of yCcP), which is poised above the sixth-coordination site of the heme iron (*45–48*). The D37K mutation breaks the hydrogen bond with His-181, altering the hydrogen-bonding network and perhaps allowing water-595 to coordinate to the heme iron. Evidence for this interpretation comes from the H181G mutant, which has a predominantly 6c-hs heme with water-595 as the most probable heme ligand (*46–48*). We can speculate that the heme-bound water in D37K is readily displaced by H_2O_2 and D37K retains 30% of its activity in spite of being six-coordinate with an A_{Soret}/A_{380} ratio of 2.59. The differential reactivity of various six-coordinate CcP species toward H_2O_2 is a second factor that may cause variation in the correlation shown in Figure 5.

A third factor that could lead to variation in the correlation between the percentage of inactive enzyme and the value of A_{Soret}/A_{380} is the method used for the estimation of inactive enzyme. As a quick screen of the ability of the mutant to react with H_2O_2 to form a Compound I-like intermediate, the spectrum of the mutant was determined in the presence and absence of a slight stoichiometric excess of H_2O_2. The assumption was made that the spectrum of the H_2O_2-oxidized mutants is identical to the spectrum of yCcP Compound I. The fractional change in the absorbance at 424 nm upon addition of H_2O_2 to the mutant compared to the change for yCcP Compound I was used as the fraction of mutant that reacted with H_2O_2. The calculated fractions of H_2O_2-inactive mutant enzyme for all 46 charge-reversal mutants are given in Tables S2 and S3 of the Supporting Information for the data at pH 6.0 and 7.5, respectively.

Even though several factors can affect the correlation between the A_{Soret}/A_{380} values and the percentage of inactive enzyme, Figure 5 is useful in showing that the six-coordinate forms tend to be less active toward H_2O_2 than the five-coordinate enzyme.

Rate of Reaction between H_2O_2 and the Charge-Reversal Mutants. The mutant enzymes were further characterized by determining their rate of reaction with H_2O_2 using stopped-flow techniques at both pH 6.0 and pH 7.5. The rate data

Scheme 1

$$\begin{array}{lcl} & \overset{k_1}{} & \\ \text{CcP(5c-hs)} + H_2O_2 & \rightarrow & \text{CcP-I} \\ k_d \uparrow\downarrow \ k_a[H_2O] & & \\ \text{CcP}\bullet H_2O & & \\ \quad \uparrow\downarrow \text{ very slow} & & \\ \text{CcP}\cdot\text{L} & & \end{array}$$

are included in Tables S2 and S3 of the Supporting Information.

The rates of the reaction with H_2O_2 could not be determined for 7 of the 46 mutants at pH 7.5 because the absorbance changes upon addition of H_2O_2 were too small to detect. Of the remaining 39 mutants, 11 gave monophasic kinetics with H_2O_2 while 28 of the mutants gave biphasic kinetics, with the slow phase of the reaction at least 10 times slower than the fast phase. The observed pseudo-first-order rate constants are defined as k_{fast} and k_{slow}. Values of k_{fast} were linearly dependent upon the H_2O_2 concentration and were generally in the range of 150 to 900 s^{-1}. Values of k_{slow} could either be linearly dependent upon the H_2O_2 concentration (19 mutants) or be independent of the H_2O_2 (10 mutants), but they were generally at least 10 times smaller than k_{fast}.

The fast phase of the H_2O_2 reaction is attributed to the bimolecular reaction between H_2O_2 and the 5c-hs form of CcP and the mutant enzymes. The slow phase of the reaction is attributed to the reaction between H_2O_2 and a six-coordinate form of CcP and the CcP mutants in which the sixth ligand is readily displaced by H_2O_2 such as water. One can accommodate all of the H_2O_2 reactivity data, including the fraction of H_2O_2-inactive enzyme, by Scheme 1.

In Scheme 1, H_2O_2 initially reacts only with that fraction of CcP present as the five-coordinate form. This gives the observed fast phase of the reaction, and if this is the only form of CcP present in solution, only the fast phase of the reaction will be observed. The observed rate constant is given by eq 4.

$$k_{fast} = k_1[H_2O_2] \quad (4)$$

The rate of equilibration between CcP(5c-hs) and CcP•H_2O is slow compared to k_{fast}, and as CcP(5c-hs) is depleted, dissociation of the water will form additional CcP(5c-hs) that reacts in the second phase of the reaction with observed rate constant k_{slow}. That fraction of CcP that does not react with H_2O_2 during the experiments must have a ligand that is not readily displaced, represented by CcP•L in Scheme 1. This ligand could be a hydroxide ion or the distal histidine. The important point is that the conversion of CcP•L to more reactive forms is very slow, much slower than the time frame of the H_2O_2 reactivity studies.

The observed rate constant for the slow phase of the reaction can be either dependent or independent of the H_2O_2 concentration depending upon the relative rates of the various reactions and the H_2O_2 concentration. After the initial depletion of CcP(5c-hs) in the fast phase of the reaction, the concentration of CcP(5c-hs) is assumed to be in a steady state determined by the competing rates of water dissociation and CcP-I formation. Under these conditions, the observed rate constant for the slow reaction is given by eq 5.

$$k_{slow} = (k_d k_1[H_2O_2])/(k_1[H_2O_2] + k_a[H_2O] + k_d) \quad (5)$$

The concentration of water in the term $k_a[H_2O]$ is a constant whether it is water-595 in the heme pocket or bulk solvent. This term can be replaced with an apparent first-order rate constant, k_b. We will also introduce the equilibrium constant for water binding, defined in eq 6, which allows us to express k_{slow} as in eq 7.

$$K_{eq} = [\text{CcP}\cdot H_2O]/[\text{CcP(5c-hs)}] = k_a[H_2O]/k_d = k_b/k_d \quad (6)$$

$$k_{slow} = (k_d k_1[H_2O_2])/(k_1[H_2O_2] + k_d K_{eq} + k_d) \quad (7)$$

For situations where $k_1[H_2O_2] \ll k_d K_{eq} + k_d$ the slow rate will be linearly dependent upon the H_2O_2 concentration as given by eq 8.

$$k_{slow} = k_1[H_2O_2]/(K_{eq} + 1) \quad (8)$$

For situations where $k_1[H_2O_2] \gg k_d K_{eq} + k_d$ the slow rate will be independent of the H_2O_2 concentration as given by eq 9.

$$k_{slow} = k_d \quad (9)$$

In Tables S2 and S3 of the Supporting Information, when the slow phase of the reaction is linearly dependent upon the H_2O_2 concentration, the value of $k_1/(K_{eq} + 1)$ is tabulated, and when the slow phase of the reaction is independent of the H_2O_2 concentration, k_d is tabulated.

At pH 7.5, 37 of the charge-reversal mutants have a component that reacts rapidly with H_2O_2. The average value of k_1 for these 37 mutants is 42 ± 7 μM^{-1} s^{-1}, comparable to the value of 45 ± 3 μM^{-1} s^{-1} determined for yCcP at pH 7.5 (*41, 50*), and we can conclude that the five-coordinate forms of the charge-reversal mutants are as reactive toward H_2O_2 as wild-type enzyme.

Nineteen of the mutants have slow phases of the reaction that are linearly dependent upon the H_2O_2 concentration, and the average value for $k_1/(K_{eq} + 1)$ is 2.7 ± 0.9 μM^{-1} s^{-1}. Ten of the mutants have slow phases that are independent of the H_2O_2 reaction, with k_d ranging in value between 6 ± 3 and 54 ± 24 s^{-1} and averaging 26 ± 18 s^{-1}.

Steady-State Velocity Measurements. We were able to detect catalytic activity for 45 of the 46 charge-reversal mutants used in this study. The internal mutant, D235K, was completely inactive toward H_2O_2 both in the H_2O_2-reactivity studies and in the steady-state catalysis studies. Forty-three of the mutants exhibit simple Michaelis–Menten behavior, characterized by a Michaelis constant, K_M, and a maximum velocity, V_{max}. The steady-state parameters are collected in Table S4 of the Supporting Information. Visual representation of K_M and V_{max}/e_0 as a function of the primary sequence position for the mutation is given in Figure 6.

Two mutants, R31E and D34K, have a biphasic dependence on the cytochrome *c* concentration with a minor phase characterized by V_{max}/e_0 and K_M values and a major phase in which the velocity increases linearly up to the highest substrate concentrations used in the study, ~100 μM ferrocytochrome *c*. The steady-state catalytic properties of R31E and D34K were reported previously (*29*). The major kinetic phase for the R31E and D34K mutants can only be characterized by giving lower limits for V_{max}/e_0 and K_M values, and these are included in Figure 6 and in Table S4 of the Supporting Information. On the basis of the lower limits for the V_{max}/e_0 values for the major phases of the

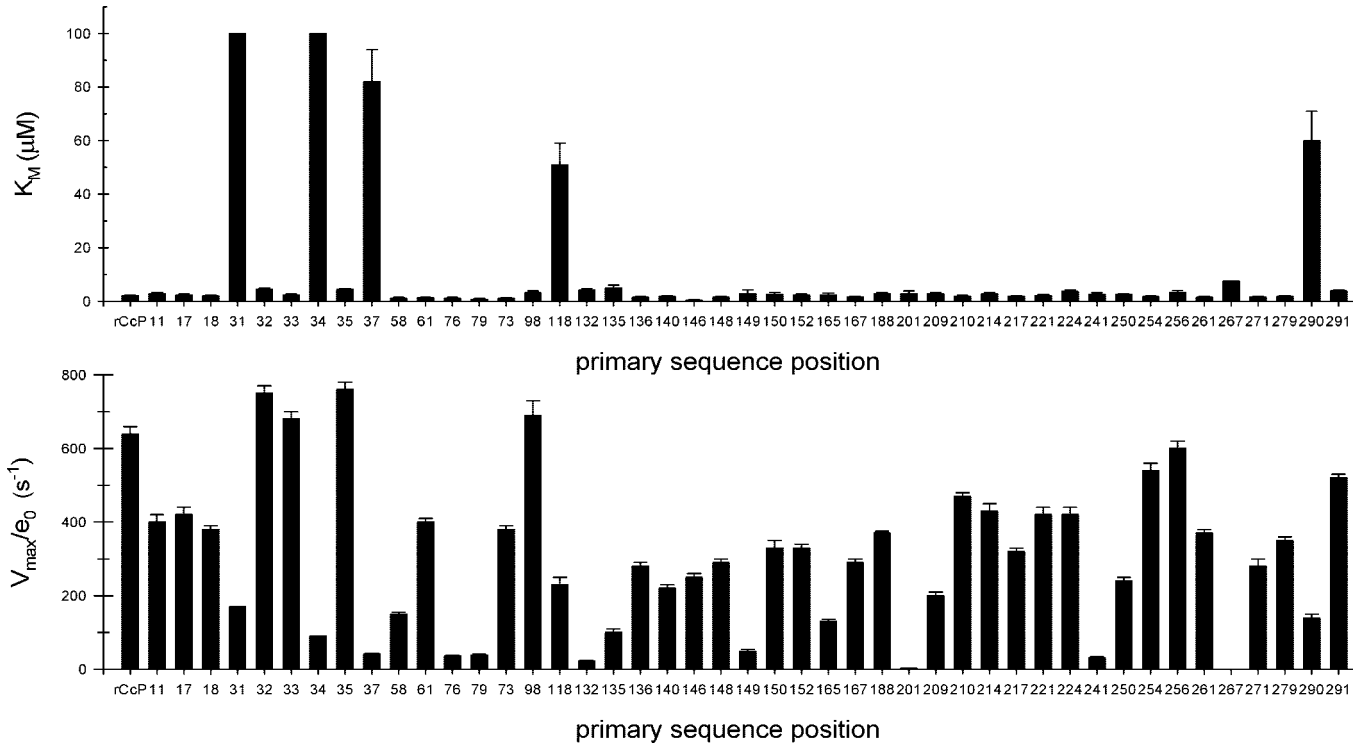

FIGURE 6: Upper panel: K_M as a function of the primary sequence position. The K_M value for rCcP is shown at the left-hand side of the top panel. Five charge-reversal mutants significantly increase the value of K_M, and these are located at primary sequence positions 31, 34, 37, 118, and 290. Lower panel: V_{max}/e_0 as a function of the primary sequence position. The V_{max}/e_0 value for rCcP is shown at the left-hand side of the lower panel.

reaction, the minor phases contribute less than 5% to the maximum activity of R31E and D34K.

Variation in V_{max}/e_0. At the beginning of these studies, we had anticipated that the charge-reversal mutations would modulate the binding affinity of cytochrome *c* to CcP but that cytochrome *c* would bind to the same site and, at saturation, would have the essentially the same maximum velocity as the wild-type enzyme. The observation of the large variation in V_{max}/e_0 (Figure 6) was unexpected. As the study progressed, it became apparent that significant fractions of some of the charge-reversal mutations were inactive toward H_2O_2 and this resulted in a significant variation in V_{max}/e_0. If we neglect the inactive mutant, D235K, and the two mutants that have biphasic kinetic behavior, R31E and D34K, V_{max}/e_0 varies over 2500-fold, from 0.3 ± 0.1 s^{-1} for E267K to 760 ± 20 s^{-1} for E35K with an average value of 314 ± 213 s^{-1}. The standard deviation for the average is indicative of the large variation of V_{max}/e_0 in the mutants. On average, the mutants are about 50% as active as the wild-type enzyme.

A major factor contributing to the variation in V_{max}/e_0 for the charge-reversal mutants is the variation in the fraction of H_2O_2-inactive enzyme documented in Figure 5 and Tables S2 and S3 (Supporting Information). A correlation between the fraction of H_2O_2-inactive enzyme and V_{max}/e_0 for the charge-reversal mutants is shown in Figure 7. Data for yCcP and rCcP are included in the figure. In general, V_{max}/e_0 decreases with increasing percentage of H_2O_2-inactive enzyme, but the correlation is not perfect. There are a number of significant downside outliers, mutants whose maximum turnover rate is much less than predicted from the fraction of H_2O_2-inactive enzyme, and a few upside outliers. This indicates that additional factors, in addition to the percentage

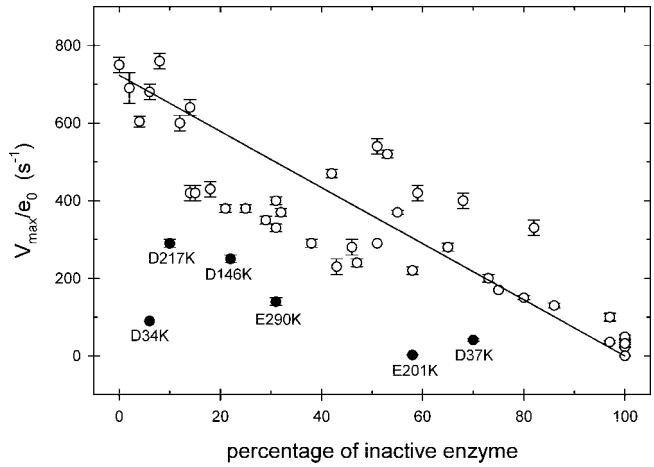

FIGURE 7: Correlation of V_{max}/e_0 and the percentage of H_2O_2-inactive enzyme at pH 7.5. Significant outliers are labeled and shown with filled circles. The correlation line is calculated by the equation $V_{max}/e_0 = (723\ s^{-1})$(fraction of active enzyme).

of H_2O_2-inactive enzyme, influence the turnover rate. Four of the downside outliers have mutations within or near the crystallographically defined cytochrome *c* binding site, and three of these, D34K, D37K, and E290K, significantly alter the binding affinity as measured by the K_M (Figure 6). It is reasonable to assume that these mutations alter the orientation of bound cytochrome *c* such that the rate of ferrocytochrome *c* oxidation is severely inhibited, leading to lower turnover rates than predicted by the percentage of enzyme that reacts with H_2O_2. These data are consistent with the idea that oxidation of ferrocytochrome *c* by CcP Compound II within the 1:1 complex, rather than product dissociation, is the rate-limiting process at 0.10 M ionic strength (*51*).

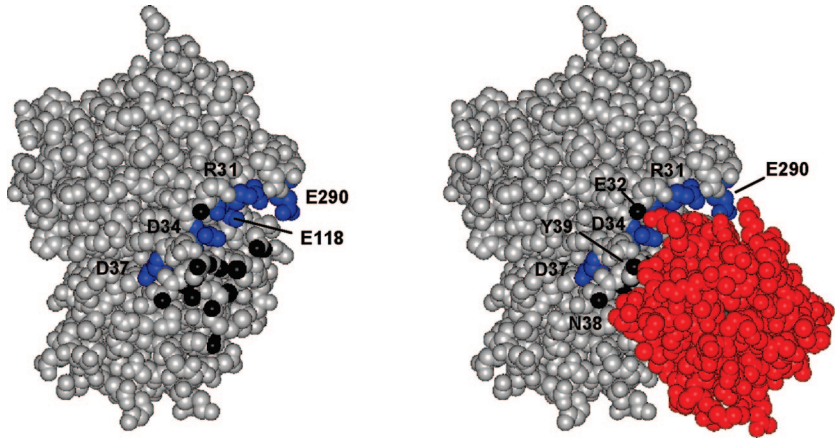

FIGURE 8: Model of CcP showing the locations of the five mutations that cause a >24-fold increase in K_M. CcP is rotated counterclockwise by 30° about a vertical axis relative to the orientation shown in Figure 1. This exposes portions of the left and front faces of CcP. D37 is not visible in Figure 1. Left panel: Only the five mutation sites (blue) are labeled in this figure, R31, D34, D37, E118, and E290. The 25 atoms that define the cytochrome *c* footprint and are visible in this orientation are unlabeled but shown in black (see Figure 1). Right panel: Same orientation as in the left panel except that bound yeast iso-1 cytochrome *c* is shown (red). Coordinates are from PCB ID 2pcc. In this representation, three of the atoms (black) defining the cytochrome *c* footprint are not covered by the bound cytochrome *c*, and their parental residues are labeled, E32, N38, and Y39.

The E201K mutant has one of the greatest effects on V_{max}/e_0, with a value of 2.8 ± 0.2 s^{-1}, less than 0.5% of rCcP. Calculation of the percent active enzyme shows that 58% of E201K reacts with H_2O_2 to form Compound I with a rate comparable to rCcP (Table S3, Supporting Information). E201K has a K_M value comparable to rCcP, suggesting that there is no alteration in binding affinity due to mutation, consistent with the crystal structure of yeast cytochrome *c*/CcP complexes (*5, 26–28*), which shows no significant electrostatic interaction between Glu-201 and any of the positively charged residues in bound cytochrome *c*. Nevertheless, residue Glu-201 is quite close to Ala-193 and Ala-194 on the surface of CcP, the putative entry point for electron transfer into CcP from cytochrome *c* within the complex (*5*). Changing the glutamate to lysine may have altered the exact orientation of the two proteins in the complex, slowing the rate of electron entry into CcP.

Two other interesting mutants are identified in Figure 7, D150K and D217K. These two mutations are far from the crystallographic cytochrome *c* binding site, have K_M values similar to rCcP, and have nearly identical V_{max}/e_0 values, 330 ± 20 and 320 ± 10 s^{-1} for D150K and D217K, respectively. However, the fractions of H_2O_2-inactive enzyme are quite different, 10% for D217K and 82% for D150K. These two mutants show the extremes in the deviation of V_{max}/e_0 values from that predicted by the correlation line in Figure 7, with D150K reacting 2.5 times faster than predicted while D217K reacts 2.2 times slower than predicted.

We believe that simple electrostatic considerations can explain most of the data shown in Figure 7 for those mutations that do not perturb the binding of cytochrome *c*. Under the conditions of the steady-state analysis, V_{max}/e_0 appears to be measuring the reduction rate of the oxyferryl, Fe(IV) group by bound ferrocytochrome *c* in the CcP Compound II/cytochrome *c* complex. Millett and colleagues (*52*) have proposed a mechanism for reduction of the Fe(IV) group in Compound II involving rapid equilibrium between two forms of Compound II, CcP-II_F, which has the oxyferryl Fe(IV) site and is the most stable form at pH 7.5, and CcP-II_R, an intermediate in which the single oxidized site in Compound II has been transferred to Trp-191, generating the π-cation radical of Trp-191. Ferrocytochrome *c* rapidly reduces the Trp-191 radical, which in turn reduces the Fe(IV) group via the rapid equilibrium. This mechanism is illustrated in Scheme 2 with V_{max}/e_0 given by eq 10.

Scheme 2

$$\begin{array}{ccc} & & k_{et} \\ \text{CcP-II}_R\cdot\text{C}^{2+} & \rightarrow & \text{CcP}\cdot\text{C}^{3+} \\ K_{CcP\text{-}II} \uparrow\downarrow & & \\ \text{CcP-II}_F\cdot\text{C}^{2+} & & \end{array}$$

$$V_{max}/e_0 = k_{et}/(K_{CcP\text{-}II} + 1) \quad (10)$$

Millett has found that k_{et} is 2×10^6 s^{-1} (*51*). $K_{CcP\text{-}II}$ would have to be about 3×10^3 to be consistent with the value of V_{max}/e_0 for wild-type CcP. This mechanism provides a reasonable explanation for the data below the correlation line in Figure 6. Just as we have suggested that the charge-reversal mutations on the surface of CcP can alter the equilibrium between five-coordinate CcP and the hydroxy-ligated form, the charge-reversal mutations could also alter the equilibrium between CcP-II_R and CcP-II_F. A negative-to-positive charge-reversal mutant would tend to destabilize the positively charged Trp-191 radical form of Compound II, increasing the value of $K_{CcP\text{-}II}$ and decreasing the value of V_{max}/e_0 as is observed for most of the mutants in Figure 7. The charge-reversal mutations would only have to change the equilibrium constant by less than a factor of 3 to explain the data in Figure 7. There are five mutations with significant positive deviations from the correlation line shown in Figure 7, and the simple electrostatic explanation does not apply. These mutants could decrease the value of $K_{CcP\text{-}II}$ for other reasons or could increase the value of k_{et} directly.

Variation in K_M for the Charge-Reversal Mutants. The primary objective of this study was to determine which of the charge-reversal mutations on the surface of CcP decreased the binding affinity for cytochrome *c* in order to map the interaction site (or sites) for cytochrome *c*. We use the K_M values from the steady-state measurements as a measure of cytochrome *c* affinity since a review of the literature shows a very good correlation between the K_M values and true

equilibrium dissociation constants, K_{D1}, for the 1:1 complex when carried out at identical conditions of ionic strength (*3, 24*). As seen in Figure 6, only five mutations cause a significant increase in the K_M, R31E, D34K, D37K, E118K, and E290K. All five of these mutations are either within or near the crystallographically defined cytochrome *c* binding site as shown in Figure 8. All five of these sites were previously identified in our report on the effect of charge-reversal mutations near the high-affinity cytochrome *c* binding site (*29*). The important new result from this study is that there are no other aspartate or glutamate residues anywhere on the surface of CcP that affect formation of the catalytically active 1:1 complex between yeast iso-1 cytochrome *c* and CcP. This effectively eliminates any model for cytochrome *c* binding that proposes multiple sites on the surface of CcP that have similar affinity for cytochrome *c*. These data also show that CcP in solution, unconstrained by crystal lattice forces, has the same cytochrome *c* binding domain as has been found in the crystalline state. This conclusion is consistent with a recent NMR study (*25*) of the CcP/yeast iso-1 cytochrome *c* complex that demonstrates the bound cytochrome has considerable mobility but generally corroborates the crystallographic structure, indicating that cytochrome *c* resides at the crystallographic site about 70% of the time and in much more dynamic encounter complexes about 30% of the time.

ACKNOWLEDGMENT

We thank Professor James Satterlee, Washington State University, for providing the plasmid containing the gene for rCcP and Professor Gary Pielak, University of North Carolina, for providing the plasmid containing the yeast iso-1 cytochrome *c* (C102T) and heme lyase genes.

SUPPORTING INFORMATION AVAILABLE

Figures describing the localization of mutation sites relative to the crystallographic cytochrome *c* binding site on CcP and figures showing the UV–visible spectra of all mutants at pH 6.0 and 7.5; in addition, tables of selected spectroscopic properties, the hydrogen peroxide reactivity at pH 6.0 and 7.5, and the steady-state parameters at pH 7.5. This material is available free of charge via the Internet at http://pubs.acs.org.

REFERENCES

1. Yonetani, T. (1966) Studies on cytochrome *c* peroxidase IV. A comparison of peroxide-induced complexes of horseradish and cytochrome *c* peroxidases. *J. Biol. Chem. 241*, 2562–2571.
2. Nocek, J. M., Zhou, J. S., De Forest, S., Priyadarshi, S., Beratan, D. N., Onuchic, J. N., and Hoffman, B. M. (1996) Theory and practice of electron transfer within protein-protein complexes: application to the multidomain binding of cytochrome *c* by cytochrome *c* peroxidase. *Chem. Rev. 96*, 2459–2489.
3. Erman, J. E., and Vitello, L. B. (2002) Yeast cytochrome *c* peroxidase: mechanistic studies via protein engineering. *Biochim. Biophys. Acta 1597*, 193–220.
4. Kang, C. H., Ferguson-Miller, S., and Margoliash, E. (1977) Steady state kinetics and binding of eukaryotic cytochromes *c* with yeast cytochrome *c* peroxidase. *J. Biol. Chem. 252*, 919–926.
5. Pelletier, H., and Kraut, J. (1992) Crystal structure of a complex between electron transfer partners, cytochrome *c* peroxidase and cytochrome *c*. *Science 258*, 1748–1755.
6. Kang, D. S., and Erman, J. E. (1982) The cytochrome *c* peroxidase-catalyzed oxidation of ferrocytochrome *c* by hydrogen peroxide. Steady state kinetic mechanism. *J. Biol. Chem. 257*, 12775–12779.
7. Northrup, S. H., Boles, J. O., and Reynolds, J. C. L. (1988) Brownian dynamics of cytochrome *c* and cytochrome *c* peroxidase association. *Science 241*, 67–70.
8. Poulos, T. L., and Kraut, J. (1980) A hypothetical model of the cytochrome *c* peroxidase cytochrome *c* electron transfer complex. *J. Biol. Chem. 255*, 10322–10330.
9. Poulos, T. L., and Finzel, B. C. (1984) Heme enzyme structure and function. *Pept. Protein Rev. 4*, 115–171.
10. Lum, V. R., Brayer, G. D., Louie, G. V., Smith, M., and Mauk, A. G. (1987) Computer modeling of yeast iso-1 cytochrome *c*-yeast cytochrome *c* peroxidase complexes. *Protein Struct., Folding, Des. 2*, 143–150.
11. Bechtold, R., and Bosshard, H. R. (1985) Structure of an electron transfer complex. II. Chemical modification of carboxyl groups of cytochrome *c* peroxidase in presence and absence of cytochrome *c*. *J. Biol. Chem. 260*, 5191–5200.
12. Stemp, E. D. A., and Hoffman, B. M. (1993) Cytochrome *c* peroxidase binds two molecules of cytochrome *c*: evidence for a low-affinity, electron-transfer-active site on cytochrome *c* peroxidase. *Biochemistry 32*, 10848–10865.
13. Mauk, M. R., Ferrer, J. C., and Mauk, A. G. (1994) Proton linkage in formation of the cytochrome *c*-cytochrome *c* peroxidase complex: electrostatic properties of the high- and low-affinity cytochrome *c* binding sites on the peroxidase. *Biochemistry 33*, 12609–12614.
14. Corin, A. F., McLendon, G., Zhang, Q., Hake, R. A., Falvo, J., Lu, K. S., Ciccarelli, R. B., and Holzschu, D. (1991) Effects of surface amino acid replacements in cytochrome *c* peroxidase on complex formation with cytochrome *c*. *Biochemistry 30*, 11585–11595.
15. Corin, A. F., Hake, R. A., McLendon, G., Hazzard, J. T., and Tollin, T. (1993) Effects of surface amino acid replacements in cytochrome *c* peroxidase on intracomplex electron transfer from cytochrome *c*. *Biochemistry 32*, 2756–2762.
16. Zhou, J. S., Tran, S. T., McLendon, G., and Hoffman, B. M. (1997) Photoinduced electron transfer between cytochrome *c* peroxidase (D37K) and Zn-substituted cytochrome *c*: probing the two-domain binding and reactivity of the peroxidase. *J. Am. Chem. Soc. 119*, 269–277.
17. Leesch, V. W., Bujons, J., Mauk, A. G., and Hoffman, B. M. (2000) Cytochrome *c* peroxidase-cytochrome *c* complex: locating the second binding domain on cytochrome *c* peroxidase with site-directed mutagenesis. *Biochemistry 39*, 10132–10139.
18. Miller, M. A. (1996) A complete mechanism for steady-state oxidation of yeast cytochrome *c* by cytochrome *c* peroxidase. *Biochemistry 35*, 15791–15799.
19. Erman, J. E., Kresheck, G. K., Vitello, L. B., and Miller, M. A. (1997) Cytochrome *c*/cytochrome *c* peroxidase complex: Effect of binding-site mutations on the thermodynamics of complex formation. *Biochemistry 36*, 4054–4060.
20. Pielak, G. J., and Wang, X. (2001) Interactions between yeast iso-1-cytochrome *c* and its peroxidase. *Biochemistry 40*, 422–428.
21. Morar, A. S., and Pielak, G. J. (2002) Crowding by trisaccharides and the 2:1 cytochrome *c*-cytochrome *c* peroxidase complex. *Biochemistry 41*, 547–551.
22. Guo, M., Bhaskar, B., Huiying, L., Barrows, T. P., and Poulos, T. L. (2004) Crystal structure and characterization of a cytochrome *c* peroxidase-cytochrome *c* site-specific cross-link. *Proc. Natl. Acad. Sci. U.S.A. 101*, 5940–5945.
23. Nakani, S., Viriyakul, T., Mitchell, R., Vitello, L. B., and Erman, J. E. (2006) Characterization of a covalently-linked yeast cytochrome *c*/cytochrome *c* peroxidase complex: Evidence for a single, catalytically-active cytochrome *c* binding site on cytochrome *c* peroxidase. *Biochemistry 45*, 9887–9893.
24. Nakani, S., Vitello, L. B., and Erman, J. E. (2006) Characterization of four covalently-linked yeast cytochrome *c*/cytochrome *c* peroxidase complexes: Evidence for electrostatic interaction between bound cytochrome *c* molecules. *Biochemistry 45*, 14371–14378.
25. Volkov, A. N., Worrall, J. A. R., Holtzmann, E., and Ubbink, M. (2006) Solution structure and dynamics of the complex between cytochrome *c* and cytochrome *c* peroxidase determined by paramagnetic NMR. *Proc. Natl. Acad. Sci. U.S.A. 103*, 18945–18950.
26. Kang, S. A., Marjavaara, P. J., and Crane, B. R. (2004) Electron transfer between cytochrome *c* and cytochrome *c* peroxidase in single crystals. *J. Am. Chem. Soc. 126*, 10836–10837.
27. Kang, S. A., and Crane, B. R. (2005) Effects of interface mutations on association modes and electron-transfer rates between protein. *Proc. Natl. Acad. Sci. U.S.A. 102*, 15465–15470.

28. Kang, S. A., Hoke, K. R., and Crane, B. R. (2006) Solvent isotope effects on interfacial protein electron transfer in crystals and electrode films. *J. Am. Chem. Soc. 128*, 2346–3355.
29. Pearl, N. M., Jacobson, T., Arisa, M., Vitello, L. B., and Erman, J. E. (2007) Effect of single-site charge-reversal mutations on the catalytic properties of yeast cytochrome *c* peroxidase: Mutations near the high-affinity cytochrome *c* binding site. *Biochemistry 46*, 8263–8272.
30. Savenkova, M. I., Satterlee, J. D., Erman, J. E., Siems, W. F., and Helms, G. L. (2001) Expression, purification, characterization, and NMR studies of highly deuterated recombinant cytochrome *c* peroxidase. *Biochemistry 40*, 12123–12131.
31. Takio, K., Titani, K., Ericsson, L. H., and Yonetani, T. (1980) Primary structure of yeast cytochrome *c* peroxidase II. The complete amino acid sequence. *Arch. Biochem. Biophys. 203*, 615–6299.
32. Teske, J. G., Savenkova, M. I., Mauro, J. M., Erman, J. E., and Satterlee, J. D. (2000) Yeast cytochrome *c* peroxidase expression in *Escherichia coli* and rapid isolation of various highly purified holoenzymes. *Protein Expression Purif. 19*, 139–147.
33. Morar, A. S., Kakouras, D., Young, G. B., Boyd, J., and Pielak, G. J. (1999) Expression of ^{15}N-labeled eukaryotic cytochrome *c* in *Escherichia coli*. *J. Biol. Inorg. Chem. 4*, 220–222.
34. Pollock, W. B. R., Rosell, F. I., Twitchett, M. B., Dumont, M. E., and Mauk, A. G. (1998) Bacterial expression of a mitochondrial cytochrome *c*. Trimethylation of Lys72 in yeast iso-1-cytochrome *c* and the alkaline conformational transition. *Biochemistry 37*, 6124–6131.
35. Drabkin, D. (1961) Analysis and interpretation of absorption spectra of haemin chromoproteins, in *Haematin Enzymes* (Falk, J. E., Lemberg, R., and Morton, R. K., Eds.)Part 1, pp 142–172,Pergamon Press Ltd., London.
36. Smith, D. W., and Williams, R. J. P. (1968) Analysis of the visible spectra of some sperm-whale ferrimyoglobin derivatives. *Biochem. J. 110*, 297–301.
37. Iizuka, T., and Yonetani, T. (1970) Spin changes in hemoproteins. *Adv. Biophys. 1*, 157–182.
38. Adar, F. (1978) Electronic absorption spectra of hemes and hemoproteins, in *The Porphyrins* (Dolphin, D., Ed.) Vol. III, pp 167–209, Academic Press, New York.
39. Yonetani, T., Wilson, D. F., and Seamonds, B. (1966) Studies on cytochrome *c* peroxidase. VIII. The effect of temperature on light absorptions of the enzyme and its derivatives. *J. Biol. Chem. 241*, 5347–5352.
40. Vitello, L. B., Huang, M., and Erman, J. E. (1990) pH-dependent spectral and kinetic properties of cytochrome *c* peroxidase: comparison of freshly isolated and stored enzyme. *Biochemistry 29*, 4283–4288.
41. Vitello, L. B., Erman, J. E., Mauro, J. M., and Kraut, J. (1990) Characterization of the hydrogen peroxide-enzyme reaction for two cytochrome *c* peroxidase mutants. *Biochim. Biophys. Acta 1038*, 90–97.
42. Dhaliwal, B. K., and Erman, J. E. (1985) A kinetic study of the alkaline transitions in cytochrome *c* peroxidase. *Biochim. Biophys. Acta 827*, 174–182.
43. Vitello, L. B., Erman, J. E., Miller, M. A., Mauro, J. M., and Kraut, J. (1992) Effect of Asp-235→Asn substitution on the absorption spectrum and hydrogen peroxide reactivity of cytochrome *c* peroxidase. *Biochemistry 31*, 11524–11535.
44. George, P., and Irvine, D. H. (1952) The reaction between metmyoglobin and hydrogen peroxide. *Biochem. J. 52*, 511–517.
45. Finzel, B. C., Poulos, T. L., and Kraut, J. (1984) Crystal structure of yeast cytochrome *c* peroxidase refined at 1.7-Å resolution. *J. Biol. Chem. 259*, 13027–13036.
46. Miller, M. A., Hazzard, J. T., Mauro, J. M., Edwards, S. L., Simons, P. C., Tollin, G., and Kraut, J. (1988) Site-directed mutagenesis of yeast cytochrome *c* peroxidase shows histidine 181 is not required for oxidation of ferrocytochrome *c*. *Biochemistry 27*, 9081–9088.
47. Mauro, J. M., Miller, M. A., Edwards, S. L., Wang, J., Fishel, L. A., and Kraut, J. (1989) Exploring structure-function relationships in yeast cytochrome *c* peroxidase using mutagenesis and crystallography, in *Metal Ions in Biological Systems* (Sigel, H., and Sigel, A., Eds.) Vol. 25, pp 477–503, Marcel Dekker, New York.
48. Miller, M. A., Shaw, A., and Kraut, J. (1994) 2.2 Å structure of oxy-peroxidase as a model for the transient enzyme:peroxide complex. *Struct. Biol. 1*, 524–531.
49. Fülöp, V., Phizackerley, R. P., Soltis, S. M., Clifton, I. J., Wakatsuki, S., Erman, J., Hajdu, J., and Edwards, S. L. (1994) Laue diffraction study on the structure of cytochrome *c* peroxidase compound I. *Structure 2*, 201–208.
50. Loo, S., and Erman, J. E. (1975) A kinetic study of the reaction between cytochrome *c* peroxidase and hydrogen peroxide. Dependence on pH and ionic strength. *Biochemistry 14*, 3467–3470.
51. Wang, K., Mei, H., Geren, L., Miller, M. A., Saunders, A., Wang, X., Waldner, J. L., Pielak, G. J., Durham, B., and Millett, F. (1996) Design of a ruthenium-cytochrome *c* derivative to measure electron transfer to the radical cation and oxyferryl heme in cytochrome *c* peroxidase. *Biochemistry 35*, 15107–15119.
52. Hahm, S., Miller, M. A., Geren, L., Kraut, J., Durham, B., and Millett, F. (1994) Reaction of horse cytochrome *c* with the radical and oxyferryl heme in cytochrome *c* peroxidase compound I. *Biochemistry 33*, 1473–1480.

BI702271R